How to cite: *Angew. Chem. Int. Ed.* **2023**, *62*, e202306135
doi.org/10.1002/anie.202306135

VIP Photocatalysis Very Important Paper

Enaminone-Linked Covalent Organic Frameworks for Boosting Photocatalytic Hydrogen Production

Xinyu Guan[+], *Yunyang Qian*[+], *Xiyuan Zhang, and Hai-Long Jiang**

Abstract: Covalent organic frameworks (COFs), possessing pre-designable structures and tailorable functionalities, are promising candidates for photocatalysis. Nevertheless, the most studied imine-linked COFs (Im-COFs) usually suffer from unsatisfactory stability and photocatalytic performance. To meet this challenge, a series of highly stable enaminone-linked COFs (En-COFs) have been synthesized and afford much improved visible-light-driven hydrogen production activities, ranging from 44 to 1078 times that of isoreticular Im-COFs, with the only difference being the linkages (enaminone vs. imine) in their structures. The enhanced light-harvesting ability, facilitated exciton dissociation and improved chemical stability account for the superior activity. Furthermore, quinoline-linked COFs (Qu-COFs) have been further obtained via the post-modification of Im-COFs. Compared with Im-COFs, the photocatalytic activities of Qu-COFs are significantly improved after modification, but still below those of the corresponding En-COFs (3–107 times). The facile synthesis, excellent activity, and high chemical stability demonstrate that En-COFs are a promising platform for photocatalysis.

Photocatalysis is widely recognized as an efficient and environmentally friendly pathway for solar-to-chemical energy conversion, in which photocatalysts play a crucial role.[1] Not limited to conventional inorganic semiconductors, in recent years, polymeric photocatalysts, including carbon nitrides,[2] conjugated microporous polymers (CMPs),[3] etc., have emerged due to their high structural diversity and adjustable band gaps. Nevertheless, traditional polymeric photocatalysts basically possess disordered structures, which are unfavorable to precise structure regulation and the corresponding mechanism study in photocatalysis. By contrast, covalent organic frameworks (COFs) are a class of crystalline porous polymers that are connected by dynamic covalent bonds.[4] Featuring periodic precise structures, high surface areas and tailorable functional groups, etc., COFs demonstrate great potential in photocatalysis.[5] Particularly, the tunable structures of COFs enable precise regulation of various parameters such as porosity, morphology and hydrophilicity, rendering them ideal platforms for exploring structure-function relationship in photocatalysis.[6]

Generally, the structures of COFs consist of two primary building units, linkers and linkages.[7] The regulation of linkers, including varying symmetries,[8] arm lengths,[9] functional groups,[10] etc., has been extensively investigated in photocatalysis. By contrast, the influence of linkages on photocatalysis has not yet been well investigated and understood, despite their critical roles in stability, light adsorption, charge separation, etc. Currently, imine and its derivatives are the most extensively studied linkages in photocatalysis; unfortunately, the moderate stability of most imine-based COFs, particularly under prolonged light irradiation, restricts their further application.[11] To alleviate this, olefin-based COFs have been developed with high conjugation and chemical durability, whereas their limited structural diversity and potential challenge in crystallization bring great difficulties in synthesis.[12] In addition, the preparation and precise structural regulation of COFs involving other linkages, such as acylhydrazone,[13] amide,[14] azo,[15] etc., remain respective challenges, and very limited studies on them have been reported thus far. In this context, it is assumed that the newly developed enaminone-linked COFs (En-COFs) might be promising alternatives due to their facile synthesis, high structural designability, and satisfactory chemical stability for advanced photocatalysis.[16]

With this in mind, a series of enaminone-linked COFs (En-COFs), named $En_{TAPT\text{-}TDOEB}$, $En_{TAPT\text{-}DDOEB}$ and $En_{DABP\text{-}TDOEB}$, have been facilely synthesized with high crystallinity and porosity (Scheme 1). Interestingly, compared with imine-linked COFs (Im-COFs, including $Im_{TAPT\text{-}TFB}$, $Im_{TAPT\text{-}TA}$ and $Im_{DABP\text{-}TFB}$), the corresponding En-COFs, featuring very similar structures except for different linkages (enaminone vs. imine) only, exhibit dramatically improved activity (44–1078 times) in photocatalytic hydrogen production. The exceptional performance of En-COFs can be attributed to their broader light adsorption, easier exciton dissociation, and improved irradiation stability. Moreover, quinoline-linked COFs (Qu-COFs, including $Qu_{TAPT\text{-}TFB}$, $Qu_{TAPT\text{-}TA}$ and $Qu_{DABP\text{-}TFB}$) were obtained via post-modification of Im-COFs to improve their photocatalytic performance.[17] Although the activities of Qu-COFs have been increased to ~2–18 times those of the corresponding Im-COFs after the modification, they still lag far behind those of En-COFs

[*] Dr. X. Guan,[+] Dr. Y. Qian,[+] X. Zhang, Prof. Dr. H.-L. Jiang
Hefei National Research Center for Physical Sciences at the Microscale, Department of Chemistry, Collaborative Innovation Center of Chemistry for Energy Materials (iChEM), University of Science and Technology of China
Hefei, Anhui 230026 (P.R. China)
E-mail: jianglab@ustc.edu.cn
Homepage: http://mof.ustc.edu.cn/

[+] These authors contributed equally to this work.

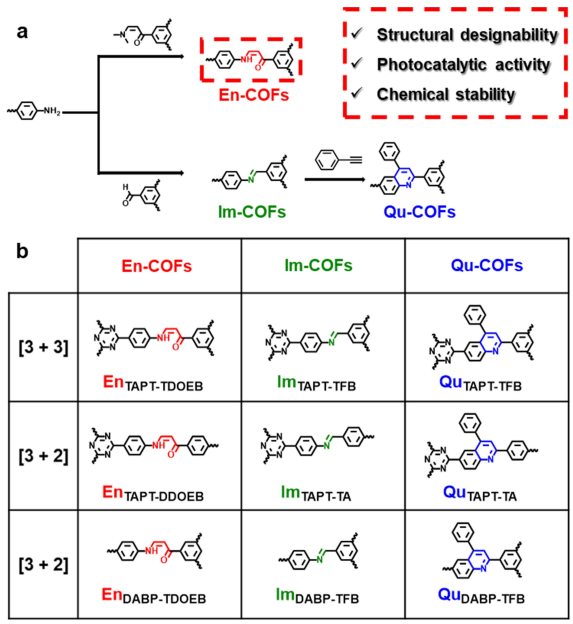

Scheme 1. a) Schematic representation of the synthetic process and the key building units of En-COFs, Im-COFs and Qu-COFs. b) Chemical structures of En-COFs, Im-COFs and Qu-COFs in this work.

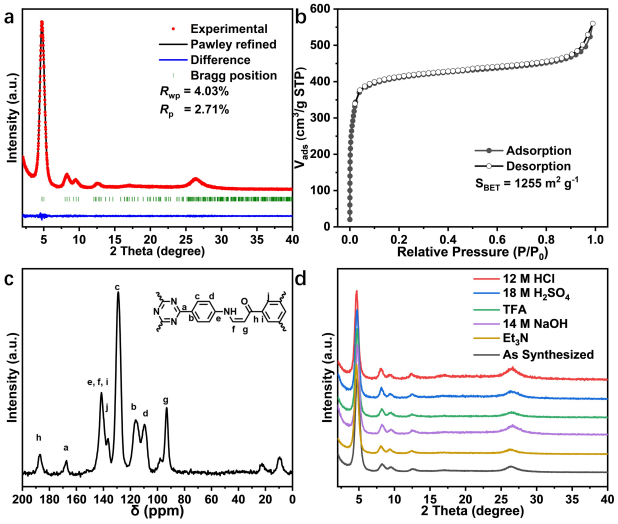

Figure 1. a) Powder XRD pattern, b) nitrogen adsorption-desorption isotherms at 77 K, and c) solid state ^{13}C NMR spectrum of $En_{TAPT\text{-}TDOEB}$. b) Powder XRD patterns of $En_{TAPT\text{-}TDOEB}$ after immersing in different acidic/alkaline conditions for 1 week.

(3.0–107 times), possibly due to the better excitonic dissociation abilities of En-COFs. To the best of our knowledge, this is the first work on enaminone-linked COFs for photocatalysis, fully manifesting their great potential.

The En-COFs were synthesized based on the conventional solvothermal method by the nucleophilic addition-elimination reaction between arylamine and enaminone monomers, as revealed by the model reaction between 3-(dimethylamino)-1-phenyl-2-propen-1-one (DPPO) and benzenamine (BA). Based on this reaction, $En_{TAPT\text{-}TDOEB}$ was synthesized with 1,3,5-tris-(4-aminophenyl)triazine (TAPT) and 1,3,5-tris(3-dimethylamino-1-oxoprop-2-enyl)benzene (TDOEB); $En_{TAPT\text{-}DDOEB}$ was synthesized with TAPT and 1,4-bi(3-dimethylamino-1-oxoprop-2-enyl)benzene (DDOEB); and $En_{DABP\text{-}TDOEB}$ was synthesized with 4,4′-diaminodiphenyl (DABP) and TDOEB (see Supporting Information, Experimental Section). For comparison, the corresponding Im-COFs with almost identical structures except for the different linkages were prepared by condensation between the arylamine and aldehyde monomers. Typically, $Im_{TAPT\text{-}TFB}$ was synthesized with TAPT and 1,3,5-triformylbenzene (TFB); $Im_{TAPT\text{-}TA}$ was synthesized with TAPT and terephthalaldehyde (TA); and $Im_{DABP\text{-}TFB}$ was synthesized with DABP and TFB (see Supporting Information, Experimental Section) .Their crystal structures were determined by powder X-ray diffraction (XRD), which revealed the same AA-stacked boron nitride nets (bnn) with hexagonal channels (*P*-6 symmetry for [3+3] structures, including $En_{TAPT\text{-}TDOEB}$ or $Im_{TAPT\text{-}TFB}$; *P*6/*m* symmetry for the other [3+2] structures, Figure 1a, S1–S5 and Table S1–S6). The predicted powder XRD patterns are highly consistent with the experimental results, along with low refinement agreement factors. Nitrogen adsorption experiments at 77 K show typical microporous characteristics with type I isotherms for both [3+3] frameworks (Figure 1b and S6), while the [3+2] structures possess type IV isotherms, indicating the characteristics of mesoporous materials (Figure S7–S10), which are consistent with the modeled crystal structures. Based on the N_2 sorption results, En-COFs exhibit moderate surface areas of 1255, 967 and 746 $m^2 g^{-1}$ for $En_{TAPT\text{-}TDOEB}$, $En_{TAPT\text{-}DDOEB}$ and $En_{DABP\text{-}TDOEB}$ (Figure 1b, S7 and S8), respectively, comparable to those of Im-COFs ranging from 854 to 1823 $m^2 g^{-1}$ (Figure S6, S9 and S10). These results indicate the similar pore features of the corresponding En-COFs and Im-COFs.

Solid-state ^{13}C cross-polarization magic-angle-spinning nuclear magnetic resonance (ssNMR) and Fourier transform infrared (FT-IR) spectra were collected for the En-COFs to well determine the chemical information of the linkages. The existence of enaminone moieties (–C-(=O)–CH=CH–N–) is evidenced by characteristic chemical shifts in ssNMR spectra at approximately 187 ppm (C=O) and 94 ppm (α-C) (Figure 1c, S11 and S12), along with IR adsorption peaks at approximately 1630 cm^{-1} (C=O), 1600 cm^{-1} (C=C) and 1180 cm^{-1} (C–N) (Figure S13 and S14). The successful synthesis can be further confirmed by the absence of signals at approximately 44 ppm (related to $N(CH_3)_2$ in enaminone monomers) in the ssNMR spectra. Similarly, imine linkages in the Im-COFs can also be manifested based on the ssNMR and FT-IR spectra (Figure S15–S18).

Given the absence of highly reversible moieties, En-COFs exhibit extremely high stability. The crystallinity and integrity of $En_{TAPT\text{-}TDOEB}$, as a representative, can be well retained in diverse organic solvents and in concentrated HCl, H_2SO_4 or NaOH solutions for 1 week (Figure 1d and S19), among the most stable COFs reported thus far (Table S7). In contrast, the corresponding $Im_{TAPT\text{-}TFB}$ be-

comes nearly amorphous in concentrated HCl, H_2SO_4 or NaOH due to the involved polarized imine linkage in the skeleton (Figure S20, S21). Subsequently, photoelectrochemical measurements have been carried out. The UV/Vis diffuse reflectance spectra of En-COFs exhibit notably red-shifted absorption edges compared to the corresponding Im-COFs, indicating the smaller band gaps (E_g) and enhanced light adsorption of the former (Figure 2a and S22–S28). Based on Mott–Schottky measurements, the lowest unoccupied molecular orbitals (LUMO), which are close to the flat bands, are determined for En-COFs and Im-COFs, and the highest occupied molecular orbitals (HOMO) are further calculated with E_g. The LUMO of En-COFs and Im-COFs are more negative than the potential for H_2O reduction (−0.4 V vs. NHE, pH 6.8), indicating their feasibility for visible-light-catalyzed H_2 evolution (Figure 2b and S29–S33). In addition, En-COFs demonstrate stronger photocurrent responses and smaller semicircles in the EIS Nyquist plots than the corresponding Im-COFs, implying better charge separation ability and lower interfacial charge transfer resistance in En-COFs (Figure 2c, d and S34–S37).

Temperature-dependent photoluminescence measurements have been further conducted to investigate the exciton dissociation kinetics, which is one of the essential factors affecting the photocatalytic activity of polymeric photocatalysts (Figure 3).[18] The integrated photoluminescence intensities increase gradually with decreasing temperature from 290 K to 80 K, and exciton binding energies (E_b) can be calculated based on the Arrhenius equation. Significantly, En-COFs present significantly lower E_b than the corresponding Im-COFs (e.g., 33.2 meV for $En_{TAPT\text{-}TDOEB}$ vs. 45.5 meV for $Im_{TAPT\text{-}TFB}$; 86.9 meV for $En_{TAPT\text{-}DDOEB}$ vs. 111.2 meV for $Im_{TAPT\text{-}TA}$; 40.4 meV for $En_{DABP\text{-}TDOEB}$ vs. 55.0 meV for $Im_{DABP\text{-}TFB}$, respectively), which clearly suggests that exciton dissociation and the generation of charge carriers are promoted in En-COFs compared with Im-COFs.

Encouraged by the aforementioned high stability, good light harvesting ability and enhanced charge separation of En-COFs, their photocatalytic performance toward H_2 production by water splitting has been investigated under visible light irradiation. As expected, En-COFs exhibit excellent activity in photocatalytic H_2 production, far superior to that of Im-COFs (Figure 4a). Specifically, the hydrogen production rates of $En_{TAPT\text{-}TDOEB}$, $En_{TAPT\text{-}DDOEB}$ and $En_{DABP\text{-}TDOEB}$ are able to reach ~2396, 675 and 734 μmol g^{-1} h^{-1}, respectively, nearly 55, 1078 and 44 times those of the corresponding Im-COFs, i.e., $Im_{TAPT\text{-}TFB}$, $Im_{TAPT\text{-}TA}$, and $Im_{DABP\text{-}TFB}$. Compared with the Im-COFs, the higher activity for these En-COFs highlights the advantage of incorporating enaminone as the COF linkage in photocatalysts. Moreover, $En_{TAPT\text{-}TDOEB}$ presents a negligible

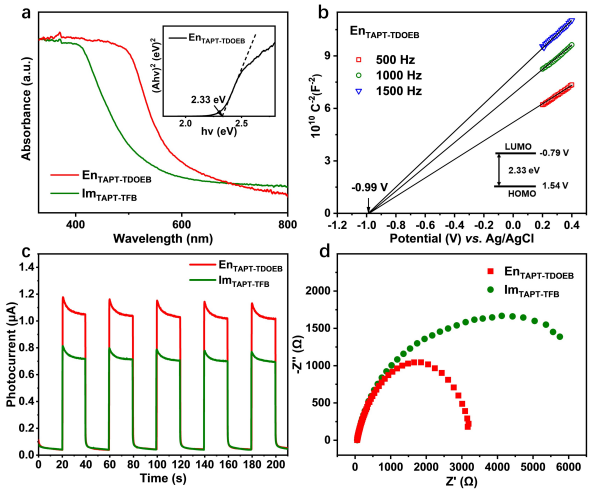

Figure 2. a) UV/Vis spectra of $En_{TAPT\text{-}TDOEB}$ and $Im_{TAPT\text{-}TFB}$. Inset: Tauc plot of $En_{TAPT\text{-}TDOEB}$. b) Mott–Schottky plots for $En_{TAPT\text{-}TDOEB}$ in 0.1 M Na_2SO_4 aqueous solution (pH 6.8). Inset: the energy diagram of the HOMO and LUMO levels of $En_{TAPT\text{-}TDOEB}$. c) Photocurrent responses and d) EIS Nyquist plots of $En_{TAPT\text{-}TDOEB}$ and $Im_{TAPT\text{-}TFB}$.

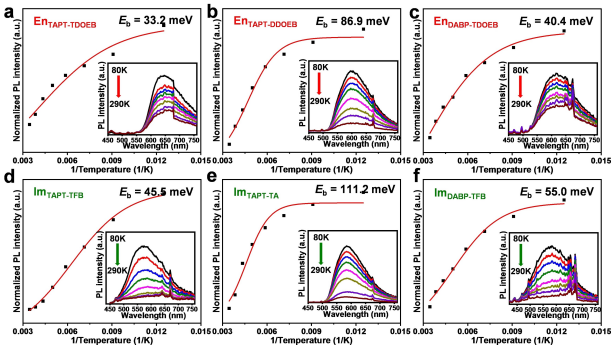

Figure 3. The intensity of photoluminescence emission (λ_{ex} = 400 nm) as a function of temperature for a) $En_{TAPT\text{-}TDOEB}$, b) $En_{TAPT\text{-}DDOEB}$, c) $En_{DABP\text{-}TDOEB}$, d) $Im_{TAPT\text{-}TFB}$, e) $Im_{TAPT\text{-}TA}$ and f) $Im_{DABP\text{-}TFB}$. Inset: temperature-dependent photoluminescence spectra from 80 K to 290 K (30 K per interval).

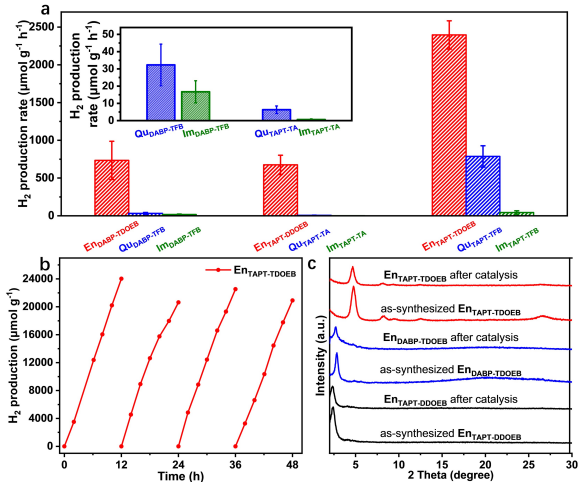

Figure 4. a) H_2 evolution rates of En-COFs, Qu-COFs and Im-COFs under visible-light irradiation ($\lambda \geq 380$ nm) in phosphate buffer (pH 7.0) in the presence of ascorbic acid as the sacrificial agent and Pt (3 wt%) as the co-catalyst (Inset: enlarged H_2 production rates of Im- and Qu-COFs). b) Four consecutive runs of photocatalytic H_2 production over $En_{TAPT\text{-}TDOEB}$ under visible light irradiation for 48 h. c) Powder XRD patterns of En-COFs before and after 2 h of photocatalysis.

activity drop in four consecutive photocatalytic runs (Figure 4b), further supporting its exceptional stability and demonstrating the good durability in photoreaction system, which are further proved by the well-retained powder XRD patterns after photocatalysis (Figure 4c). Unfortunately, the powder XRD intensities of all the Im-COFs decrease significantly after photocatalysis under similar conditions (Figure S38), well supporting the much higher stability and superiority of En-COFs in photocatalysis.

To improve the poor photocatalytic activity and chemical stability of Im-COFs, the corresponding Qu-COFs have been fabricated via post-modification of the Im-COFs (Scheme 1). Similar powder XRD patterns illustrate the retained framework topology after post-modification (Figure S39–S41), and the successful linkage transformation from imine to quinoline can be well proved by ^{13}C ssNMR and FT-IR spectra (Figure S42–S45). Upon such a post-modification, the enhanced conjugation of the resulting Qu-COFs can be significantly increased, giving rise to their improved light harvesting (Figure S46–S51), exciton dissociation ability (Figure S52–S54), and chemical stability (Figure S55, S56), compared with the parent Im-COFs. Meanwhile, Qu-COFs are able to preserve suitable band structures for visible-light photocatalytic hydrogen production (Figure S57–S59). As a result, the photocatalytic H_2 production rates could reach ~787, 6 and 32 $\mu mol\,g^{-1}\,h^{-1}$ for $Qu_{TAPT\text{-}TFB}$, $Qu_{TAPT\text{-}TA}$ and $Qu_{DABP\text{-}TFB}$, respectively, which are ~18, 10 and 2 times that of the corresponding Im-COFs (Figure 4a). To our surprise, despite the significant improvement achieved after post-modification, the photocatalytic activity of all the Qu-COFs still falls short when compared to En-COFs (Figure 4a). The superior activity of En-COFs might be attributed to the facilitated exciton dissociation, as evidenced by the lower E_b (Figure 3 and S52–S54), preliminarily manifesting their particularly outstanding potential among COFs in photocatalysis.

In summary, we have successfully prepared three enaminone-linked COFs (En-COFs) with exceptional chemical stability for photocatalytic H_2 production. The corresponding Im-COFs involving basically the same building units yet imine linkages, a class of intensively studied COFs, have been deliberately synthesized as controls. Moreover, the imine linkage in Im-COFs has been further post-synthetically modified to obtain Qu-COFs with extended light harvesting and enhanced stability for further comparison. Remarkably, though this is the first study on photocatalysis over En-COFs, they demonstrate excellent activity in photocatalytic H_2 production under visible light irradiation, exponentially higher than those of corresponding Im-COFs and Qu-COFs, possibly due to accelerated exciton dissociation and promoted charge separation. Moreover, the En-COFs are able to maintain their crystallinity and photocatalytic activities under long-term light irradiation, while the Im-COFs largely lose their crystallinity after photocatalysis. Given the facile synthesis, good light adsorption, tailorable structures, exceptional stability, and particularly strong exciton dissociation ability, we believe that these enaminone-linked COFs might be an excellent platform for enhanced photocatalysis.

Acknowledgements

This work was supported by the National Key Research and Development Program of China (2021YFA1500400), Strategic Priority Research Program of the CAS (XDB0450302), NSFC (22205224 and 22161142001), China Postdoctoral Science Foundation (BX2021281 and 2021M703064), and Fundamental Research Funds for the Central Universities (WK2060000041).

Conflict of Interest

The authors declare no conflict of interest.

Data Availability Statement

The data that support the findings of this study are available from the corresponding author upon reasonable request.

Keywords: Covalent Organic Frameworks · Enaminone Linkage · Excitonic Effects · Photocatalysis

[1] Q. Wang, K. Domen, *Chem. Rev.* **2020**, *120*, 919–985.
[2] a) X. Wang, K. Maeda, A. Thomas, K. Takanabe, G. Xin, J. M. Carlsson, K. Domen, M. Antonietti, *Nat. Mater.* **2009**, *8*, 76–80; b) L. Lin, Z. Yu, X. Wang, *Angew. Chem. Int. Ed.* **2019**, *58*, 6164–6175.
[3] a) Y. Wang, A. Vogel, M. Sachs, R. S. Sprick, L. Wilbraham, S. J. A. Moniz, R. Godin, M. A. Zwijnenburg, J. R. Durrant, A. I. Cooper, J. Tang, *Nat. Energy* **2019**, *4*, 746–760; b) Y. Xu, S. Jin, H. Xu, A. Nagai, D. Jiang, *Chem. Soc. Rev.* **2013**, *42*, 8012–8031; c) Z. Zhang, J. Jia, Y. Zhi, S. Ma, X. Liu, *Chem. Soc. Rev.* **2022**, *51*, 2444–2490; d) C. Zhao, Z. Chen, R. Shi, X. Yang, T. Zhang, *Adv. Mater.* **2020**, *32*, 1907296; e) L. Yang, Y. Peng, X. Luo, Y. Dan, J. Ye, Y. Zhou, Z. Zou, *Chem. Soc. Rev.* **2021**, *50*, 2147–2172.
[4] a) A. P. Côté, A. I. Benin, N. W. Ockwig, M. O'Keeffe, A. J. Matzger, O. M. Yaghi, *Science* **2005**, *310*, 1166–1170; b) J. Feng, Y.-J. Zhang, S.-H. Ma, C. Yang, Z.-P. Wang, S.-Y. Ding, Y. Li, W. Wang, *J. Am. Chem. Soc.* **2022**, *144*, 6594–6603; c) R. L. Li, A. Yang, N. C. Flanders, M. T. Yeung, D. T. Sheppard, W. R. Dichtel, *J. Am. Chem. Soc.* **2021**, *143*, 7081–7087; d) Q. Zhang, S. Dong, P. Shao, Y. Zhu, Z. Mu, D. Sheng, T. Zhang, X. Jiang, R. Shao, Z. Ren, J. Xie, X. Feng, B. Wang, *Science* **2022**, *378*, 181–186; e) C. Kang, Z. Zhang, A. K. Usadi, D. C. Calabro, L. S. Baugh, K. Chai, Y. Wang, D. Zhao, *J. Am. Chem. Soc.* **2022**, *144*, 20363–20371; f) T. Zhang, G. Zhang, L. Chen, *Acc. Chem. Res.* **2022**, *55*, 795–808; g) L. Deng, Z. Ding, X. Ye, D. Jiang, *Acc. Mater. Res.* **2022**, *3*, 879–893.
[5] a) L. Stegbauer, K. Schwinghammer, B. V. Lotsch, *Chem. Sci.* **2014**, *5*, 2789–2793; b) A. Jati, K. Dey, M. Nurhuda, M. A. Addicoat, R. Banerjee, B. Maji, *J. Am. Chem. Soc.* **2022**, *144*, 7822–7833; c) X. Kan, J.-C. Wang, Z. Chen, J.-Q. Du, J.-L. Kan, W.-Y. Li, Y.-B. Dong, *J. Am. Chem. Soc.* **2022**, *144*, 6681–6686; d) Y.-N. Gong, X. Guan, H.-L. Jiang, *Coord. Chem. Rev.* **2023**, *475*, 214889; e) S. Yang, W. Hu, X. Zhang, P. He, B. Pattengale, C. Liu, M. Cendejas, I. Hermans, X. Zhang, J. Zhang, J. Huang, *J. Am. Chem. Soc.* **2018**, *140*, 14614–14618; f) W. Zhou, Q.-W. Deng, H.-J. He, L. Yang, T.-Y. Liu, X. Wang, D.-Y. Zheng, Z.-B. Dai, L. Sun, C. Liu, H. Wu, Z. Li,

W.-Q. Deng, *Angew. Chem. Int. Ed.* **2023**, *62*, e202214143; g) N. Keller, T. Bein, *Chem. Soc. Rev.* **2021**, *50*, 1813–1845; h) P. T. Parvatkar, S. Kandambeth, A. C. Shaikh, I. Nadinov, J. Yin, V. S. Kale, G. Healing, A.-H. Emwas, O. Shekhah, H. N. Alshareef, O. F. Mohammed, M. Eddaoudi, *J. Am. Chem. Soc.* **2023**, *145*, 5074–5082; i) Y. Fan, D. W. Kang, S. Labalme, J. Li, W. Lin, *Angew. Chem. Int. Ed.* **2023**, *62*, e202218908; j) W. Huang, N. Huber, S. Jiang, K. Landfester, K. A. I. Zhang, *Angew. Chem. Int. Ed.* **2020**, *59*, 18368–18373.

[6] a) W. Zhang, L. Chen, S. Dai, C. Zhao, C. Ma, L. Wei, M. Zhu, S. Y. Chong, H. Yang, L. Liu, Y. Bai, M. Yu, Y. Xu, X.-W. Zhu, Q. Zhu, S. An, R. S. Sprick, M. A. Little, X. Wu, S. Jiang, Y. Wu, Y.-B. Zhang, H. Tian, W.-H. Zhu, A. I. Cooper, *Nature* **2022**, *604*, 72–79; b) S. Zhang, G. Cheng, L. Guo, N. Wang, B. Tan, S. Jin, *Angew. Chem. Int. Ed.* **2020**, *59*, 6007–6014; c) W. Liu, X. Li, C. Wang, H. Pan, W. Liu, K. Wang, Q. Zeng, R. Wang, J. Jiang, *J. Am. Chem. Soc.* **2019**, *141*, 17431–17440.

[7] C. S. Diercks, O. M. Yaghi, *Science* **2017**, *355*, eaal1585.

[8] a) K. Wang, X. Kang, C. Yuan, X. Han, Y. Liu, Y. Cui, *Angew. Chem. Int. Ed.* **2021**, *60*, 19466–19476; b) Y. Meng, Y. Luo, J.-L. Shi, H. Ding, X. Lang, W. Chen, A. Zheng, J. Sun, C. Wang, *Angew. Chem. Int. Ed.* **2020**, *59*, 3624–3629.

[9] a) K. Xiong, Y. Wang, F. Zhang, X. Li, X. Lang, *Appl. Catal. B* **2023**, *322*, 122135; b) Q. Zhi, W. Liu, R. Jiang, X. Zhan, Y. Jin, X. Chen, X. Yang, K. Wang, W. Cao, D. Qi, J. Jiang, *J. Am. Chem. Soc.* **2022**, *144*, 21328–21336; c) M. Liu, K. Jiang, X. Ding, S. Wang, C. Zhang, J. Liu, Z. Zhan, G. Cheng, B. Li, H. Chen, S. Jin, B. Tan, *Adv. Mater.* **2019**, *31*, 1807865.

[10] a) M. Lu, M. Zhang, J. Liu, T.-Y. Yu, J.-N. Chang, L.-J. Shang, S.-L. Li, Y.-Q. Lan, *J. Am. Chem. Soc.* **2022**, *144*, 1861–1871; b) Y. Qian, D. Li, Y. Han, H.-L. Jiang, *J. Am. Chem. Soc.* **2020**, *142*, 20763–20771; c) Z. Zhao, Y. Zheng, C. Wang, S. Zhang, J. Song, Y. Li, S. Ma, P. Cheng, Z. Zhang, Y. Chen, *ACS Catal.* **2021**, *11*, 2098–2107; d) C. Krishnaraj, H. S. Jena, L. Bourda, A. Laemont, P. Pachfule, J. Roeser, C. V. Chandran, S. Borgmans, S. M. J. Rogge, K. Leus, C. V. Stevens, J. A. Martens, V. V. Speybroeck, E. Breynaert, A. Thomas, P. V. D. Voort, *J. Am. Chem. Soc.* **2020**, *142*, 20107–20116; e) J. Xu, C. Yang, S. Bi, W. Wang, Y. He, D. Wu, Q. Liang, X. Wang, F. Zhang, *Angew. Chem. Int. Ed.* **2020**, *59*, 23845–23853.

[11] a) T. Banerjee, F. Podjaski, J. Kröger, B. P. Biswal, B. V. Lotsch, *Nat. Rev. Mater.* **2021**, *6*, 168–190; b) C. Qian, L. Feng, W. L. Teo, J. Liu, W. Zhou, D. Wang, Y. Zhao, *Nat. Chem. Rev.* **2022**, *6*, 881–898; c) L. Cusin, H. Peng, A. Ciesielski, P. Samorì, *Angew. Chem. Int. Ed.* **2021**, *60*, 14236–14250; d) P. Das, G. Chakraborty, J. Roeser, S. Vogl, J. Rabeah, A. Thomas, *J. Am. Chem. Soc.* **2023**, *145*, 2975–2984; e) X. Xu, P. Cai, H. Chen, H.-C. Zhou, N. Huang, *J. Am. Chem. Soc.* **2022**, *144*, 18511–18517; f) H. Lin, C. Chen, T. Zhou, J. Zhang, *Sol. RRL* **2021**, *5*, 2000458; g) P.-F. Wei, M.-Z. Qi, Z.-P. Wang, S.-Y. Ding, W. Yu, Q. Liu, L.-K. Wang, H.-Z. Wang, W.-K. An, W. Wang, *J. Am. Chem. Soc.* **2018**, *140*, 4623–4631.

[12] a) E. Jin, M. Asada, Q. Xu, S. Dalapati, M. A. Addicoat, M. A. Brady, H. Xu, T. Nakamura, T. Heine, Q. Chen, D. Jiang, *Science* **2017**, *357*, 673–676; b) S. Xu, M. Richter, X. Feng, *Acc. Mater. Res.* **2021**, *2*, 252–265; c) S. Li, R. Ma, S. Xu, T. Zheng, H. Wang, G. Fu, H. Yang, Y. Hou, Z. Liao, B. Wu, X. Feng, L.-Z. Wu, X.-B. Li, T. Zhang, *ACS Catal.* **2023**, *13*, 1089–1096.

[13] S. Yang, R. Sa, H. Zhong, H. Lv, D. Yuan, R. Wang, *Adv. Funct. Mater.* **2022**, *32*, 2110694.

[14] Z. Li, J.-a. Wang, S. Ma, Z. Zhang, Y. Zhi, F. Zhang, H. Xia, G. Henkelman, X. Liu, *Appl. Catal. B* **2022**, *310*, 121335.

[15] Z.-B. Zhou, P.-J. Tian, J. Yao, Y. Lu, Q.-Y. Qi, X. Zhao, *Nat. Commun.* **2022**, *13*, 2180.

[16] Y. Liu, Y. Wang, H. Li, X. Guan, L. Zhu, M. Xue, Y. Yan, V. Valtchev, S. Qiu, Q. Fang, *Chem. Sci.* **2019**, *10*, 10815–10820.

[17] X. Li, C. Zhang, S. Cai, X. Lei, V. Altoe, F. Hong, J. J. Urban, J. Ciston, E. M. Chan, Y. Liu, *Nat. Commun.* **2018**, *9*, 2998.

[18] a) H. Wang, S. Jin, X. Zhang, Y. Xie, *Angew. Chem. Int. Ed.* **2020**, *59*, 22828–22839; b) F. Liu, Y. He, X. Liu, Z. Wang, H.-L. Liu, X. Zhu, C.-C. Hou, Y. Weng, Q. Zhang, Y. Chen, *ACS Catal.* **2022**, *12*, 9494–9502; c) W. Wang, H. Wang, X. Tang, J. Huo, Y. Su, C. Lu, Y. Zhang, H. Xu, C. Gu, *Chem. Sci.* **2022**, *13*, 8679–8685; d) C. Li, J. Liu, H. Li, K. Wu, J. Wang, Q. Yang, *Nat. Commun.* **2022**, *13*, 2357; e) Z.-A. Lan, G. Zhang, X. Chen, Y. Zhang, K. A. I. Zhang, X. Wang, *Angew. Chem. Int. Ed.* **2019**, *58*, 10236–10240.

Manuscript received: May 2, 2023
Accepted manuscript online: May 31, 2023
Version of record online: June 23, 2023